PULSAR SPIN-DOWN BY A FALLBACK DISK AND THE P-$\dot{P}$ DIAGRAM

M. ALİ ALPAR

Faculty of Engineering and Natural Sciences, Sabancı University, Orhanlı-Tuzla, Istanbul 81474, Turkey

AND

AŞKIN ANKAY AND EFE YAZGAN

Department of Physics, Middle East Technical University, Ankara 06531, Turkey

ABSTRACT

Neutron stars may be surrounded by fallback disks formed from supernova core collapse. If the disk circumscribes the light cylinder, the neutron star will be an active radio pulsar spinning down under the propeller spin-down torque applied by the disk as well as the usual magnetic dipole radiation torque. Evolution across the P-$\dot{P}$ diagram is very rapid when pulsar spin-down is dominated by the propeller torque. This explains the distribution of pulsars in the P-$\dot{P}$ diagram.

Subject headings: pulsars: general — stars: neutron

1. INTRODUCTION

Efforts to understand the newly identified classes of neutron stars, in particular anomalous X-ray pulsars (AXPs; Mereghetti 2001) and soft gamma-ray repeaters (SGRs; Woods et al. 1999), have followed two avenues. Magnetar models, involving neutron star dipole magnetic fields $B \sim 10^{14}$–10^{15} G, above the quantum critical field $B_c = m^2 c^3/e\hbar = 4.4 \times 10^{13}$ G, were advanced to explain the mechanism and energetics of SGRs (Thompson & Duncan 1995). Alternative models propose to explain the new classes of neutron stars in terms of conventional $B \sim 10^{12}$ G fields. These models involve accretion or propeller (Illarionov & Sunyaev 1975) torques from an accretion disk surrounding the isolated neutron stars (Alpar 1999, 2001; Chatterjee, Hernquist, & Narayan 2000). Alpar (1999, 2001) argued that radio pulsars, dim thermal neutron stars (DTNSs; Treves et al. 2000), AXPs and radio-quiet neutron stars (RQNSs; Chakrabarty et al. 2001), and perhaps SGRs represent alternative pathways of young neutron stars, distinguished by the history of mass inflow ($\dot{M}$) from a fallback accretion disk. This work classified young neutron stars according to ranges of $\dot{M}$, taken as representative constant values, with radio pulsars corresponding to zero or very weak $\dot{M}$, such that the disk does not quench the pulsar magnetosphere. The inner radius of the disk must lie at or beyond the light cylinder. Disks around radio pulsars were first proposed by Michel & Dessler (1981, 1983) and Michel (1988). For the AXPs, Chatterjee et al. (2000) studied a fallback disk with a specific time-dependent mass inflow rate $\dot{M}(t)$ taken to follow a self-similar thin-disk solution, which entails a power-law decay of $\dot{M}(t)$ (Cannizzo, Lee, & Goodman 1990; Mineshige, Nomoto, & Shigeyama 1993). According to this model, some neutron stars go through propeller and accretion (AXP) phases as $\dot{M}(t)$ evolves while others, at magnetic fields less than 3×10^{12} G, become radio pulsars after a very brief initial accretion phase.

What are the implications of a fallback disk for radio pulsars? Marsden, Lingenfelter, & Rothschild (2001a, 2001b) argued that the presence of a propeller spin-down torque from a fallback disk in conjunction with the magnetic dipole radiation torque may explain the large discrepancy (Gaensler & Frail 2000) between the real (kinematic) age and the "characteristic" age $P/2\dot{P}$ corresponding to pure dipole spin-down for the pulsar B1757−24 and that pulsar–supernova remnant (SNR) age discrepancies can be explained in a similar way. Menou, Perna,

& Hernquist (2001b) showed that this combination of dipole and propeller torques can explain the braking indexes $n < 3$ of five young pulsars.

In this Letter, we apply the combined spin-down torque, using the model of Menou et al. (2001b), to the distribution of pulsars in the P-$\dot{P}$ diagram. The presence of torques other than dipole radiation torques, in particular torques that might arise from the ambient medium near a young pulsar in an SNR, was proposed first by Yusifov et al. (1995) to explain qualitatively the measured braking indexes $n < 3$ of young pulsars, the discrepancy between real and characteristic ages, and the distribution of pulsars in the P-$\dot{P}$ diagram. Gvaramadze (2001) invokes torques from circumstellar clumps in the SNR to derive a "true" age for PSR B1509−58 in agreement with the SNR age. In § 2, we explore the combined torque model, using the canonical magnetic dipole torque together with the model of Menou et al. (2001b) for the propeller spin-down torque, with a constant mass inflow rate $\dot{M}$. Evolutionary tracks in the P-$\dot{P}$ diagram are presented in § 3 along with analytical expressions for time spans of various phases, braking indexes, and other properties of the tracks. The P-$\dot{P}$ diagram is divided into strips delineated by tracks of constant magnetic field and mass inflow rate. Each strip is divided into period bins, and a histogram is constructed for the number of pulsars in each period bin. A curve for the expected number of pulsars as a function of period is calculated according to the model and compared with the histogram for each strip. The results are discussed in § 4.

2. SPIN-DOWN OF A PULSAR WITH A FALLBACK DISK

We model the spin-down of a pulsar under the combined action of magnetic dipole radiation and propeller spin-down torques as

$$I\Omega\dot{\Omega} = -\beta\Omega^4 - \gamma, \tag{1}$$

adopting the model of Menou et al. (2001b) with their notation. The neutron star will continue to act as a radio pulsar as long as the fallback disk does not protrude into the light cylinder. If the disk were detached from the light cylinder, it would not exert any torque on the neutron star and its magnetosphere. Assuming that the disk is attached to the light cylinder, the

torque can be estimated as

$$N_{disk} = -2\dot{M}r_{lc}^2[\Omega - \Omega_K(r_{lc})] \cong -2\dot{M}r_{lc}^2\Omega$$

$$= -2\dot{M}c^2/\Omega \equiv -\gamma/\Omega, \quad (2)$$

where $\dot{M}$ is the mass inflow rate interacting with the light cylinder and being ejected from the disk; $r_{lc} = c/\Omega$ is the light cylinder radius, and $r_{lc}^2\Omega$ is the specific angular momentum extracted from the pulsar magnetosphere, since the Keplerian rotation rate $\Omega_K(r_{lc})$ in the disk is small compared with the rotation rate Ω of the neutron star and its magnetosphere. The parameter $\gamma = 2\dot{M}c^2 = 2 \times 10^{31}\dot{M}_{10}$ ergs s^{-1} is the rate of energy loss of the neutron star due to the propeller torque; $\dot{M}_{10}$ is the mass inflow rate in units of 10^{10} g s^{-1}. The rate of energy loss due to magnetic dipole radiation is given by

$$\dot{E}_{dipole} = -B_\perp^2 R^6 \Omega^4/6c^3 = -\beta\Omega^4. \quad (3)$$

Here $B_\perp$ is the component of the dipole magnetic field at the neutron star surface in the direction perpendicular to the rotation axis and R is the neutron star radius. This defines $\beta = 6.17 \times 10^{27}B_{\perp,12}^2 R_6^6$. Menou et al. (2001b) give the solution of equation (1) for constant $\dot{M}$ as

$$t = \tau\{\arctan[(\beta/\gamma)^{1/2}\Omega_i^2] - \arctan[(\beta/\gamma)^{1/2}\Omega(t)^2]\} \quad (4)$$

$$= \tau\{\pi/2 - \arctan[(\beta/\gamma)^{1/2}\Omega(t)^2]\},$$

where Ω_i, the initial rotation rate of the pulsar, is always large enough to justify the second equation. The timescale τ is $\tau = I/2(\gamma\beta)^{1/2} = 4.5 \times 10^7\dot{M}_{10}^{-1/2}B_{\perp,12}^{-1}$ yr. In the P-$\dot{P}$ diagram, pulsars will follow tracks given by equation (1),

$$\dot{P} = (4\pi^2\beta/I)P^{-1} + (\gamma/4\pi^2I)P^3. \quad (5)$$

Menou et al. (2001b) have used this model to explain the observed values of the braking index $n = \ddot{\Omega}\Omega/\dot{\Omega}^2$. From their model we derived ($\dot{M}$, $B_\perp$) values (2.8×10^{16} g s^{-1}, 7.1×10^{12} G) for the Crab pulsar, (1.5×10^{16} g s^{-1}, 8.9×10^{12} G) for PSR B0540−69, (1.4×10^{15} g s^{-1}, 5.2×10^{12} G) for the Vela pulsar, (2.8×10^{13} g s^{-1}, 8×10^{13} G) for PSR J1119−6127, and (3.6×10^{14} g s^{-1}, 3×10^{13} G) for PSR B1509−58.[1]

3. THE DISTRIBUTION OF PULSARS IN THE P-$\dot{P}$ DIAGRAM

We used P and $\dot{P}$ data from the Princeton Pulsar Catalog (Taylor, Manchester, & Lyne 1993).[2] Tracks corresponding to equation (5) are shown in Figure 1. At early times (small P), the dipole term dominates and the pulsar follows the left branch of the track, essentially spinning down under the magnetic dipole radiation torque. The braking index for pure dipole spin-down is $n = 3$, and the left branch of each track follows the slope $n' = 2 - n = -1$ in the log $\dot{P}$–log P diagram,

$$P\dot{P} = (4\pi^2\beta/I) \propto B_\perp^2. \quad (6)$$

[1] The magnetic field of PSR J1119−6127 is $B_\perp = 8.2 \times 10^{13}$ G if one assumes dipole spin-down. Camilo et al. (2000) report $B_\perp = 4.1 \times 10^{13}$ G in the discovery paper because of a missing factor of $\frac{1}{2}$ in the definition of the neutron star's dipole moment.
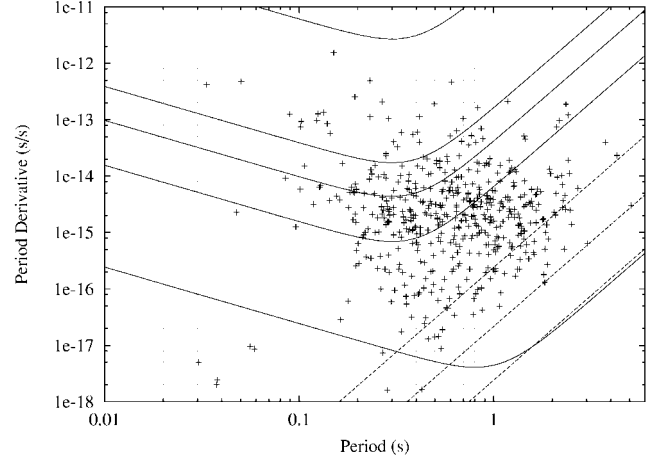[2] See http://pulsar.ucolick.org/cog/pulsars/catalog.

FIG. 1.—The log P (s)–log $\dot{P}$ (s s^{-1}) diagram. Strips used for the histograms in Fig. 2 are separated by the tracks shown, (Fig. 2a) $B_{\perp,12} = 50$–4, (Fig. 2b) $B_{\perp,12} = 4$–2, (Fig. 2c) $B_{\perp,12} = 2$–0.8, and (Fig. 2d) $B_{\perp,12} = 0.8$–0.1. The dashed lines are death lines $B_{\perp,12}/P^2 = \alpha$ for (left to right) $\alpha = 1$, 0.3, and 0.1.

The transition to the regime in which the propeller torque dominates occurs at the minimum of a track, at the period

$$P_0 = (2\pi)(\beta/3\gamma)^{1/4} = 2\pi/\Omega_0. \quad (7)$$

The slope $n' = 0$, and the braking index $n = 2$ at this point. The minimum value of the spin-down rate is found to be

$$\dot{P}_{min} = (4\pi^2\beta/I)P_0^{-1} + (\gamma/4\pi^2I)P_0^3 = (8\pi/I)\gamma^{1/4}(\beta/3)^{3/4}. \quad (8)$$

The propeller spin-down torque is dominant along the right branch of each track. The asymptotic behavior, reached already at periods of about $2P_0$, has the slope $n' = 3$ ($n = -1$). The evolution is very rapid on this branch. Neutron stars will spin down to $\Omega = 0$ ($P = \infty$) in a finite time:

$$t_{max} = \pi\tau/2 = 7 \times 10^7\dot{M}_{10}^{-1/2}B_{\perp,12}^{-1} \text{ yr.} \quad (9)$$

One-third of this time is spent before reaching the minimum $\dot{P}$ at P_0. About $0.23t_{max}$ is spent before reaching $n = 2.5$, $P = (3/7)^{1/4} \cong 0.8P_0$, when the pulsar has started deviating from dipole spin-down. The evolution slows down at periods around the turning point at P_0 to $P = \sqrt{3}P_0$, $n = 0$. From $n = 2.5$, $P \cong 0.8P_0$ to $P = \sqrt{3}P_0$, $n = 0$, it takes $0.44t_{max}$. As the pulsar proceeds into the propeller spin-down branch, the evolution speeds up, as $\dot{P} \propto P^3$; spin-down from $P = \sqrt{3}P_0$ to $P = \infty$ takes only $t_{max}/3$.

Pulsar activity will turn off upon reaching a critical voltage (the "death lines," the "death valley") at a period satisfying $B_{\perp,12}/P^2 = \alpha = 0.1$–1 (see Fig. 1). The propeller spin-down tracks are parallel to the death lines. In our analysis of the P-$\dot{P}$ diagram, we find that the minimum mass inflow rate for the pulsars in our sample is $\dot{M}_{min} = 4.5 \times 10^8$ g s^{-1}. The propeller spin-down track for $\dot{M}_{min}$ bounds the pulsar population on the right and is of the form $B_{\perp,12}/P^2 = 0.3$. This track is already in the death valley. Pulsars with $\dot{M} < \dot{M}_{min}$ will reach the death valley and turn off while they are still on the dipole spin-down track. Pulsars with $\dot{M} > \dot{M}_{min}$ will evolve on their propeller spin-

down tracks until they reach $P_{death} = (B_{\perp, 12}/\alpha)^{1/2}$ at an age

$$t_{death} = t_{max}\{[1 - (2/\pi) \arctan [0.7\alpha(\dot{M}_{10})^{-1/2}]]\}. \quad (10)$$

This age for pulsar turnoff is close to t_{max} for almost all cases. Even for the track at $\dot{M}_{min}$ with $\alpha = 0.3$, we find $t_{death} = 0.5t_{max}$. At times close to t_{max}, evolution is rapid. Few pulsars are observed at late times (long periods) along the propeller spin-down tracks. Therefore, pulsar turnoff will not effect the distribution of pulsars in the P-$\dot{P}$ diagram except for the lowest $\dot{M}$. The spin-down lifetime t_{max} is plausible in view of the low $\dot{M}$ values obtained for the pulsar tracks. A time-dependent disk would reach $\dot{M} \approx 10^8$–10^{10} g s^{-1} on timescales $\sim 10^8$ yr. If the disk is depleted before the pulsar completes its evolution, the pulsar will switch to the pure dipole spin-down track corresponding to its magnetic field.

The number ΔN of pulsars with magnetic field $B_{\perp}$ and mass inflow rate $\dot{M}$ in a period interval ΔP at period P is

$$\Delta N = [\Delta N(P; \ \beta, \ \gamma)/\Delta P]\Delta P$$
$$= Rf(P, \dot{P})[\Delta t(P; \ \beta, \ \gamma)/\Delta P]\Delta P$$
$$= Rf(P, \dot{P})[\dot{P}(P; \ \beta, \ \gamma)]^{-1}\Delta P. \quad (11)$$

Here R is the birthrate of pulsars in the Galaxy, and $f(P, \dot{P})$, the fraction of the galactic disk volume in which pulsars of period P and period derivative $\dot{P}$ are observable, describes selection effects. For simplicity, we take $f(P, \dot{P})$ to be constant, assuming that the variation in $f(P, \dot{P})$ is negligible compared with the variation of $\dot{P}$. We further assume that one and only one track (β, γ) passes through each point in the P-$\dot{P}$ plane, such that the plane can be divided into strips separated by chosen (β, γ) tracks. For each strip, we count the pulsars in equal-sized period bins and construct the histogram of ΔN. We then choose a representative track $(\bar{\beta}, \bar{\gamma})$ for the strip such that the function $\Delta N(P) = $ constant$/\dot{P}(P; \ \bar{\beta}, \bar{\gamma})$ matches the histogram.

The combined dipole and propeller spin-down model has a minimum $\dot{P}$ at the period P_0 on each track. $\Delta N \propto \dot{P}^{-1}$ must have a maximum at P_0; this is where a pulsar's motion across the P-$\dot{P}$ diagram is slowest. The model predicts that $\Delta N \propto \dot{P}^{-1}$ will increase in proportion to P at short periods and decrease in proportion to P^{-3} at $P > P_0$. The histograms do have this property. For each strip, we fit the histogram by choosing $\bar{\beta}$ to have the average value for the strip and choosing $\bar{\gamma}$ such that P_0 is in the period bin with the maximum number ΔN_{max} of pulsars. The normalization of the model curve is chosen to match the histogram at $(P_0, \Delta N_{max})$. Four strips separated by boundary tracks with $B_{\perp, 12} = 50, 4, 2, 0.8$, and 0.1 are shown on the P-$\dot{P}$ diagram in Figure 1. For the upper four boundary tracks, $P_0 = 0.3$ s, and for the lowest boundary track at $B_{\perp, 12} = 0.1$, $P_0 = 0.8$ s.

4. RESULTS AND DISCUSSION

The number distribution of pulsars in the P-$\dot{P}$ plane is fitted remarkably well with the combined effect of dipole and propeller spin-down. The mass inflow rates range from a few times 10^{16} g s^{-1} for the youngest pulsars to a minimum of 4.5×10^8 g s^{-1}. The histograms for the four strips shown in Figure 2 show reasonable agreement with representative model curves. The model curves representing the four strips are characterized

by $B_{\perp, 12} = 35.5$, $P_0 = 0.15$ s (Fig. 2a); $B_{\perp, 12} = 3.16$, $P_0 = 0.3$ s (Fig. 2b); $B_{\perp, 12} = 1.52$, $P_0 = 0.3$ s (Fig. 2c); and $B_{\perp, 12} = 0.57$, $P_0 = 0.8$ s (Fig. 2d). The agreement with the model is not sensitive to the choice of strip boundaries except for $B_{\perp, 12} < 0.4$, where a second peak appears in the histograms at $P \simeq 1.3$ s, as seen in Figure 2d. This excess may reflect disk depletion resulting in pulsars dropping down from many propeller spin-down tracks at higher $B_{\perp}$ and $\dot{M}$ to their corresponding pure dipole spin-down tracks at periods close to death lines.

P_0 is found to vary between 0.15 and 0.8 s. From equation (7), the limited range of P_0 suggests a correlation between B and $\dot{M}$. Such a correlation is not expected physically. It arises because a model with constant $\dot{M}$ is used to represent the real spin-down, which occurs under a time-dependent $\dot{M}(t)$. The period P_0 reflects the value of $\dot{M}$ at time t_0, when $\dot{P}$ is minimum. To understand the effect in a simple way, suppose that at $P_0(t_0)$ the dipole and propeller torques experienced by the pulsar are equal. Suppose the mass inflow rate follows a power-law decay $\dot{M}(t) \propto t^{-\eta}$. The pulsar is initially evolving down its dipole spin-down track, with $P(t) \propto t^{1/2}$. We can define a $P_0(t) = P_0[\beta, \dot{M}(t)]$, the turning point into the propeller track, according to the current $\dot{M}(t)$. From equation (7), $P_0(t) = 2\pi[\beta/3\gamma(t)]^{1/4} \propto t^{\eta/4}$. For early times, $P(t) < P_0(t)$. One can imagine the pulsar moving along its dipole track with $P(t) \propto t^{1/2}$ while the junction with the propeller track at the current $\dot{M}(t)$ moves down the dipole track, ahead of the pulsar but at a slower rate $P_0(t) \propto t^{\eta/4}$. At $t = t_0$, $P(t_0) = P_0(t_0)$, and the pulsar is just turning into its current propeller track. For $t > t_0$, the pulsar follows its current propeller track while the track itself continues to shift toward the bottom right corner of the P-$\dot{P}$ diagram, as $\dot{M}(t)$ continues to decrease. To derive the form of $\dot{M}(t)$, let us use the observation that $P_0(t_0) = P_0[\beta, \dot{M}(t_0)]$ is similar for all pulsars. Taking $P_0 = 0.3$ s gives $\dot{M}(t_0) = 1.98 \times 10^{11}B_{\perp, 12}^2$. Dipole spin-down (eq. [6]) until $t = t_0$ yields $P_0 = 1.23 \times 10^{-4}B_{\perp, 12}t_0$ (yr)$^{1/2} = 0.3$ s, or $B_{\perp, 12}^2 = 5.95 \times 10^6/t_0$ (yr). Thus, we find that $\dot{M}(t) = 1.18 \times 10^{18}$ (g s^{-1}) t (yr)$^{-1}$, that is, $\eta = 1$. For $B_{\perp, 12} = 1$, $t_0 = 5.95 \times 10^6$ yr and $\dot{M}(t_0) \cong 2 \times 10^{11}$ g s^{-1} are obtained.

The application here to all pulsars across the P-$\dot{P}$ diagram and its success in fitting the pulsar distribution require and support the presence of low-mass, low-$\dot{M}$ disks, which are active for pulsar lifetimes of the order of 10^7 yr and remain attached to the light cylinder. The time dependence of the disk and the mass inflow rate it supplies could be incorporated in a more detailed calculation. The self-similar isolated thin-disk models with a power-law decay of $\dot{M}(t)$ were employed by Menou et al. (2001b), who point out that, for the Crab pulsar, PSR B0540−09 and PSR B1509−58, thin disks in the $\dot{M}$ ranges indicated by the braking indexes of these pulsars are consistent with observational constraints in the optical although most of the disk luminosity would be in the UV, where detections are much harder. For the Vela pulsar, only a very small and highly inclined disk could be compatible with observational constraints. According to the classification of Alpar (2001), disks are present around all classes of young neutron stars, providing accretion for AXPs and acting as propellers on DTNSs and RQNSs. For two AXPs and the RQNS in Cas A, luminosities predicted by thin-disk models are ruled out or tightly constrained by observations in the optical and IR (Coe & Pightling 1998; Hulleman et al. 2000b; Hulleman, van Kerkwijk, & Kulkarni 2000a; Kaplan, Kulkarni, & Murray 2001). It is likely that disks under propeller boundary conditions are not standard thin disks (Alpar 2001). As the mass inflow is
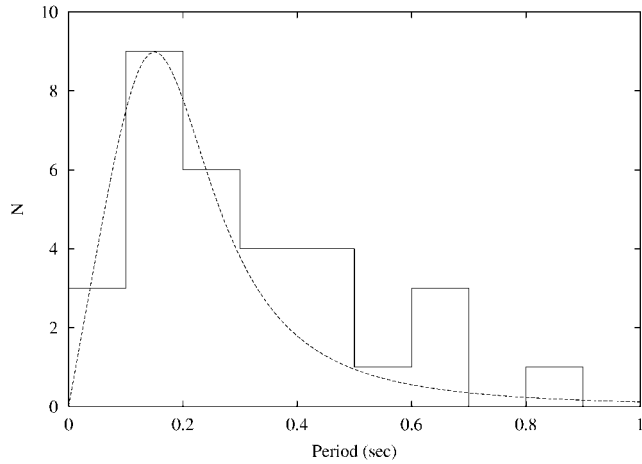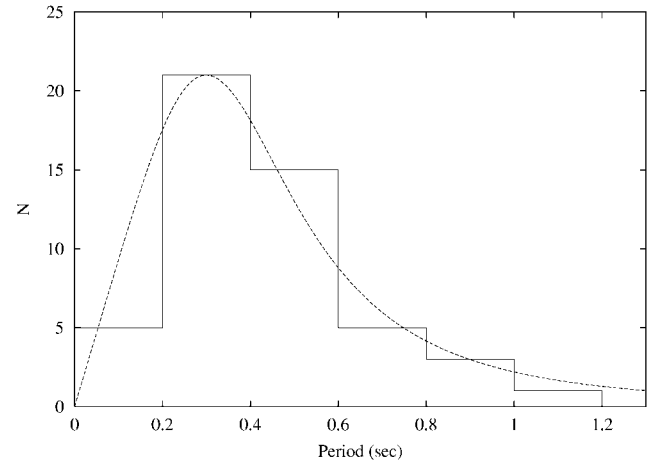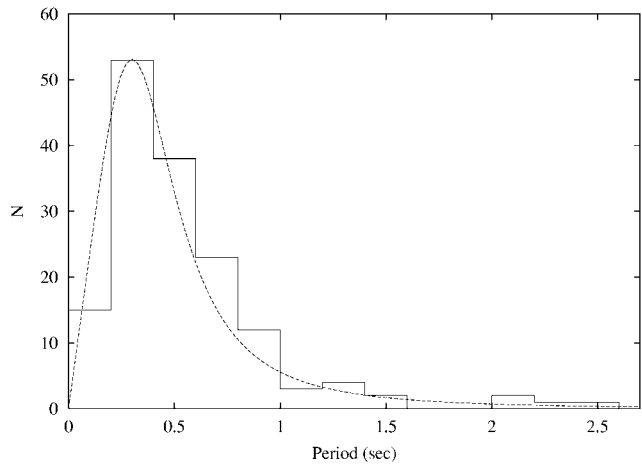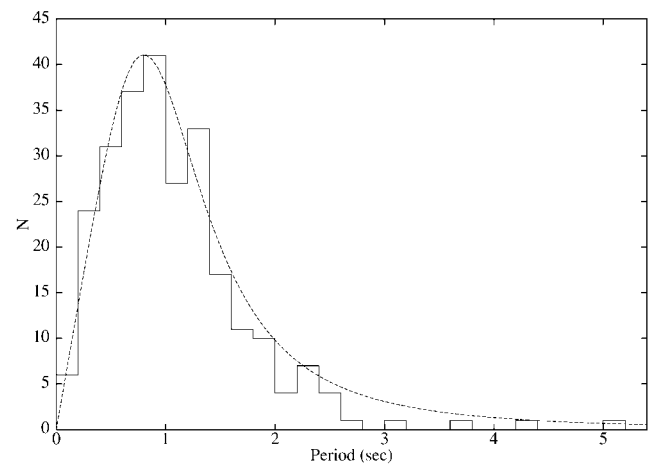
FIG. 1a

FIG. 1b

FIG. 1c

FIG. 1d

FIG. 2.—Histograms showing the number of pulsars in period bins for each of the strips shown in Fig. 1. The model curve on each histogram is drawn for the average $\beta \propto B_{\perp,12}^2$ for the strip, with $\gamma \propto \dot{M}$ chosen such that the maximum of the histogram occurs at $P_0 = 2\pi(\beta/3\gamma)^{1/4}$.

stopped at the disk-magnetosphere boundary and largely ejected from the system, the disk may be enshrined in a corona and outflow of ejected matter, possibly with larger effective area and different spectrum. Menou, Perna, & Hernquist (2001a) have shown that the thin disks may become neutral and stop evolving as thin disks. The transition would quench the disk's luminosity, but it would also suppress the dynamical evolution of the disk if the viscosity of MHD origin is no longer operational. However, a smaller but nonzero viscosity should be operating in a neutral disk. Furthermore, irradiation by the pulsar will probably keep the disk ionized and allow the mass inflow to continue, possibly as a power-law decay. The minimum rotational energy loss rate of the pulsars is of the order of 10^{30} ergs s^{-1}. The luminosity of the irradiated disk may be shifted to different spectral bands (Perna & Hernquist 2000).

The present application to the P-$\dot{P}$ diagram shows no indication of an effect on the pulsar distribution due to depletion of the disk before pulsar turnoff, except possibly for the oldest pulsars, well advanced in their evolution on propeller spin-down tracks, dropping down to pure dipole tracks near death lines. This may indicate that there is no separate disk timescale. Disks interacting with pulsars via propeller torques may be driven by these torques to evolve on the propeller spin-down timescales of the pulsars. These problems, as well as the as-

sumption that the disk remains attached to the light cylinder, require further work on the coupling between the disk and the pulsar magnetosphere. A Monte Carlo simulation of the P-$\dot{P}$ diagram will test the present model with independent random distributions of B and $\dot{M}$ and selection effects.

We predict that some pulsars have braking indexes less than 2, like the Vela pulsar (though the $n = 1.4 \pm 0.2$ braking index measurement for this pulsar should be treated with some caution because its timing behavior is dominated by interglitch relaxation). About $\frac{2}{3}$ of all pulsars will be on the propeller spin-down branch, with $n < 2$, at $P > P_0$. One-half of these pulsars will have negative braking indexes, $-1 < n < 0$. Measurement of braking indexes is unfortunately very difficult since the timing behavior is dominated by noise (Baykal et al. 1999) and, it seems, also by interglitch recovery (M. A. Alpar & A. Baykal 2001, in preparation).

The model also predicts very small numbers $\Delta N \propto P^{-3}$ of the oldest pulsars, which have long periods and large $\dot{P}$ values. These pulsars would give magnetic fields $B_{\perp} \sim 10^{12}$–10^{13}, perhaps 10^{14} G with the combined dipole-propeller spin-down model. For these pulsars the pure dipole spin-down model would yield higher fields, extending into the magnetar range, and young ages. Thus, kinematic age measurements of pulsars with long periods and large $\dot{P}$ can distinguish between pure

dipole spin-down and propeller spin-down. Propeller spin-down also increases the rate of energy dissipation in pulsars and in neutron stars evolving under propeller torques after pulsar activity is over.

REFERENCES

Alpar, M. A. 1999, preprint (astro-ph/9912228)
———. 2001, ApJ, 554, 1245
Baykal, A., Alpar, M. A., Boynton, P. E., & Deeter, J. E. 1999, MNRAS, 306, 207
Camilo, F., Kaspi, V. M., Lyne, A. G., Manchester, R. N., Bell, J. F., D'Amico, N., McKay, N. P. F., & Crawford, F. 2000, ApJ, 541, 367
Canizzo, J. K., Lee, H. M., & Goodman, J. 1990, ApJ, 351, 38
Chakrabarty, D., Pivovaroff, M. J., Hernquist, L. E., Heyl, J. S., & Narayan, R. 2001, ApJ, 548, 800
Chatterjee, P., Hernquist, L., & Narayan, R. 2000, ApJ, 534, 373
Coe, M. J., & Pightling, S. L. 1998, MNRAS, 299, 223
Gaensler, B. M., & Frail, D. A. 2000, Nature, 406, 158
Gvaramadze, V. V. 2001, A&A, 374, 259
Hulleman, F., van Kerkwijk, M. H., & Kulkarni, S. R. 2000a, Nature, 408, 689
Hulleman, F., van Kerkwijk, M. H., Verbunt, F. W. M., & Kulkarni, S. R. 2000b, A&A, 358, 605
Illarionov, A. F., & Sunyaev, R. A. 1975, A&A, 39, 185
Kaplan, D. L., Kulkarni, S. R., & Murray, S. S. 2001, ApJ, in press (astro-ph/0102054)

Marsden, D., Lingenfelter, R. E., & Rothschild, R. E. 2001a, ApJ, 547, L45
———. 2001b, preprint (astro-ph/0102049)
Menou, K., Perna, R., & Hernquist, L. 2001a, ApJ, in press (astro-ph/0102478)
———. 2001b, ApJ, in press (astro-ph/0103326)
Mereghetti, S. 2001, in The Neutron Star–Black Hole Connection, ed. C. Kouveliotou, J. van Paradijs, & J. Ventura (NATO ASI Ser.; Dordrecht: Kluwer), in press (astro-ph/9911252)
Michel, F. C. 1988, Nature, 333, 644
Michel, F. C., & Dessler, A. J. 1981, ApJ, 251, 654
———. 1983, Nature, 303, 48
Mineshige, S., Nomoto, K., & Shigeyama, T. 1993, A&A, 267, 95
Perna, R., & Hernquist, L. 2000, ApJ, 544, L57
Taylor, J. H., Manchester, R. N., & Lyne, A. G. 1993, ApJS, 88, 529
Thompson, C., & Duncan, R. C. 1995, MNRAS, 275, 255
Treves, A., Turolla, R., Zane, S., & Colpi, M. 2000, PASP, 112, 297
Woods, P. M., et al. 1999, ApJ, 519, L139
Yusifov, I. M., Alpar, M. A., Gök, F., & Guseinov, O. H. 1995, in The Lives of the Neutron Stars, ed. M. A. Alpar, Ü. Kızıloğlu, & J. van Paradijs (NATO ASI Ser. C, 450; Dordrecht: Kluwer), 201